Innovative blade shape for micro wind turbines

Aurélien Carré, Émile Roux, Laurent Tabourot, Pierre Gasnier

Innovative blade shape for micro wind turbines

Aurélien Carré
Université Savoie Mont Blanc, SYMME,
F-74000 Annecy, France
aurelien.carre@univ-smb.fr

Émile Roux
Université Savoie Mont Blanc, SYMME,
F-74000 Annecy, France
emile.roux@univ-smb.fr

Laurent Tabourot
Université Savoie Mont Blanc, SYMME,
F-74000 Annecy, France
laurent.tabourot@univ-smb.fr

Pierre Gasnier
Université Grenoble Alpes, CEA-LETI, MINATEC,
F-38000 Grenoble, France
pierre.gasnier@cea.fr

***Abstract*—This study reports the design and fabrication of innovative blades for a centimeter-scale propeller and the experimental testing of a wind harvester. A samara wing structure is taken as a model to optimize the aerodynamics at low Reynolds number. The performances of the 44 mm diameter horizontal-axis micro wind turbine are tested in two dedicated wind tunnels, with wind speeds from 1.2 m.s^{-1} to 8 m.s^{-1}. The output electrical powers range from 50 μW to 80 mW, with a maximal overall efficiency of 17.5% for 4 m.s^{-1}. It appears that this bioinspired prototype have better performances than almost all the previous studies on small-scale wind harvesters in a large wind speeds range, and gives hope to get even higher.**

***Index Terms*—Energy harvesting, Micro wind turbine, Low wind speeds, Biomimetics**

I. Introduction

Wireless Sensor Nodes (WSN) are used for a large type of measures (temperature, humidity, presence, vibrations or even CO2 concentration) and are usually powered by batteries: this requires a periodical maintenance with inevitable costs, especially if the WSN is located in a difficult-to-access area. In order to avoid it, some developments are now made in the field of energy harvesting with Micro Electro-Mechanical Systems (MEMS). The sources are varied: water or air flows, vibrations, light... If we look at the power density of the energy source, compared to batteries, air flows appear to be interesting even at low wind speeds (down to 1 m.s^{-1}) [1].

Airflow-driven energy harvesters, and more particularly horizontal-axis wind turbines, exploit the power of the air, which is expressed as:

$$P_{air} = \frac{1}{2}\rho S U_0^3, \tag{1}$$

with ρ the air density, S the rotor cross-section and U_0 the air speed upstream of the system. The output electrical power is then: $P_{elec} = \eta_{gene}.C_P.P_{air}$, with C_P the power coefficient of the turbine, which is limited to around 59% because of the Betz limit, and η_{gene} the generator efficiency. The overall efficiency of the harvester is thus: $\eta = C_P.\eta_{gene}$.

For small systems (1 m diameter and less), the overall efficiency can go from 30% for a 1.26 m rotor diameter [2], [3], to 20% for 40 cm [4]–[7], down to around 0.4% for the smallest and less efficient system [8]. Electromagnetic generators are often used for mechanical to electrical conversion. They are more used than electrostatic technologies due to their better power density [9].

In this paper, we will focus on centimeter-scale horizontal wind turbines with a rotor diameter of around 7 cm and less. Since the beginning of the 2000s, some great studies have been made in this field. From 2 to 7.2 cm of diameter, with a working wind speed between 2 to 11.8 m.s^{-1}, the output electrical powers for different harvesters in the literature range from 0.5 to 227.4 mW [10]–[17]. The maximum overall efficiencies η for each device and for our prototype are listed in Table I.

TABLE I
Overview of the maximum efficiency of existing harvesters

Reference	Rotor diameter	Maximal efficiency	Maximal electrical power
[10]	7.2 cm	15%	102.61 mW at 8 m.s^{-1}
[11]	6.3 cm	8%	9.95 mW at 4.7 m.s^{-1}
[12]	4.5 cm	8%	69.9 mW at 10 m.s^{-1}
[13]	4.2 cm	9.5%	130 mW at 11.8 m.s^{-1}
[14]	3.5 cm	28%	24.6 mW at 7 m.s^{-1}
[15]	3.45 cm	12%	4.5 mW at 4 m.s^{-1}
[16]	2.6 cm	3.2%	5.6 mW at 8.8 m.s^{-1}
[17]	2 cm	3.9%	4.32 mW at 10 m.s^{-1}
This work	4.4 cm	17.5%	80 mW at 8 m.s^{-1}

It can be noticed that, except for the very interesting result of Gasnier et al. in 2019 with an overall efficiency reaching 28%, the other harvesters highlight an issue in the process of extreme miniaturization: only 15% of the wind power is extracted in the best case. This is mainly due to the low Reynolds number close to the blades in these low wind speed conditions. Moreover, the lowest cut-in speed is 1.5 m.s^{-1}, which has to be improved to exploit even lower wind speeds.

The Reynolds number for a blade with a chord c, under a wind speed U_0 with ν the cinematic viscosity of the air is:

$$Re = \frac{U_0.c}{\nu} \tag{2}$$

In the case of centimeter-scale harvesters, c and U_0 are very small, giving Re around $10^3 - 10^4$, which characterizes a laminar (or low turbulent) flow. The lift-to-drag ratio of the blades is then way beyond the ones seen on large scale; consequently, the wind turbine will be less efficient than a

larger one [2]. The main goal is thus to find a new blade design at small dimensions with better aerodynamical properties, in order to optimize the power coefficient of the propeller and thus the overall efficiency of the harvester. As an example, Kunz et al. mentioned in 2003 that it is possible to optimize the lift-to-drag ratio, even at small scale, in particular with the use of thin and cambered blades [18].

A radically different method is to use biomimicry: in a numerical study by Holden et al. published in 2015, the mechanical efficiency (or power coefficient C_P) of a maple seed is evaluated during its rotational movement. The results show a value of 59%, very close to the maximum being the Betz limit at 59.3% [19]. Therefore, in the present study, it is chosen to follow this path and to develop it.

II. Biomimetic conception of the propeller

A. Cinematics of a maple seed

The natural specimens with movement that come closest to micro turbine rotors are maple seeds, also called samaras. Their length is comprised between 1 and 18 cm [20], and they are composed of a dry fruit and a wing.

During their fall from a tree, the combination of the two parts creates an autorotation that permits the seed to land far from its initial point. This rotation is measured to be between 80 and 150 rad.s^{-1}, or between 760 and 1430 rev.min^{-1}, and the fall speed is around 1 m.s^{-1} [20], [21]. Moreover, the Reynolds number of samaras blades during their rotation is found to be around $10^3 - 10^4$ [22], [23]. All those parameters are interestingly close to what can be observed for the working conditions of centimeter-scale wind harvesters at low wind speeds [14].

Thanks to those results, maple seeds are taken as models for a new design of turbine blades at small dimensions. The aim is thus to copy their shape, with the best precision possible.

B. Reverse engineering and fabrication

The first step towards reverse engineering is to scan a samara to get its geometry. If possible, a 3D scan permits to have the entire volume. Here, it was only possible to measure one face of a samara. The seed was stuck to a plane and the position of around 3 000 000 points were measured. The result of the scan is shown on Fig. 1.

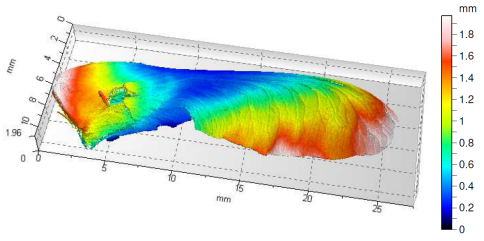

Fig. 1. Scan of the samara with colors representing the height of the points.

One can notice that the seed is globally curved: this is why the center is blue and the extremities are red or white. Moreover, the hole in the middle of the seed is intentional. The most interesting part is the undulation that can be seen on the trailing edge of the wing: the colors are between orange and white, so the points on this area are between 1.3 and 1.9 mm in height. This shows an important curvature in the wing structure relatively to the thickness, which gives the samara its particular aerodynamic properties [19].

Thus, this undulation is reproduced in the design of the blades for the turbine rotor, as well as the outer contour of the samara and the thickness of the different parts. Fig. 2 proposes a view of the reconstructed model from below.

Fig. 2. View of the wing undulation in the CAD reconstruction.

For the fabrication of the propeller, it is chosen to use stereolithography (SLA) which is a type of additive manufacturing. Machining and molding processes were discarded because of the complexity of implementation for this type of parts. The SLA technique is chosen mostly thanks to its precision of fabrication, which in our case with a Formlabs Form 2 printer is about 100 μm. However, the tiny veins on the wing that can be seen on the scan on Fig. 1 are too small to be replicated: the wing is then flattened, keeping only the undulation. Moreover, the manufacturing precision is not sufficient to have the real thickness of the samara: this one is measured at 0.1 mm. A few parts printed with this thickness show badly manufactured or deteriorated areas and encourage to thicken the wing a bit; the final CAD model is then designed with 0.4 mm for the wing, to keep a thin structure and to ensure a good fabrication.

C. Complete harvester

In order to make a propeller based on the samara design, the previous CAD model is cut to remove the most massive part, corresponding to the seed. The wing is then linked to an 8 mm diameter hub and is duplicated to make a variable number of blades. Two angles can also be changed: the pitch angle (noted α_p) and the coning angle (noted β). The pitch angle is inducted by the blade rotation along its own axis; it impacts its angle of attack. The coning angle is the one between the rotation plane of the propeller and the blade axis; it is observed on samaras during their autorotation. Depending on the coning angle value, the propeller diameter is about 44 mm.

For the mechanical to electrical conversion, a micro permanent magnet generator is used. It is made of a samarium-cobalt (SmCo) cylindrical magnet, which presents a good remanent induction, and a copper wire wrapped around it. The magnet is fixed to a rotated shaft, this one being supported by two micro ceramic bearings to minimize the friction. A coreless generator is chosen because of its low starting torque that is better for low wind speeds. The outer dimensions of the generator are $14\times11\times25$ mm^3. The propeller with eight blades and the electromagnetic generator are represented on Fig. 3.

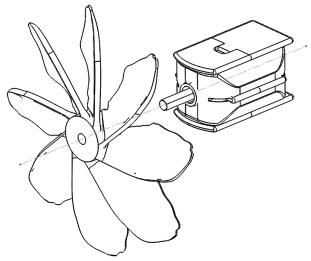

Fig. 3. The complete harvester: a bioinspired propeller and a micro generator.

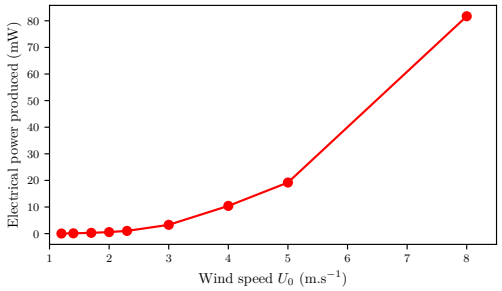

Fig. 4. Maximum output power for each wind speed tested.

III. Experimental results

A. Testing materials

In order to characterize the harvester on a large band of wind speeds, two different wind tunnels are used: a first one for "low speeds", from 0.5 to 2.3 m.s^{-1}, and a second one for "high speeds" between 3 and 8 m.s^{-1}. A test at 2.3 m.s^{-1} has been made with both to confirm that the results are equivalent. Moreover, to guarantee a good flow quality, the harvester rotor area is verified to be less than 2% of the two tunnels areas.

In order to measure the electrical power produced, the generator is connected to a variable resistive load, which value R_{load} is set between 5 Ω and 90 kΩ during the tests. An oscilloscope is connected in parallel to the load to measure the voltage: its own impedance (1 MΩ) is taken into account, giving an equivalent resistive load R_{eq}. The output power of the harvester P_{elec} is therefore the power dissipated by Joule effect in the load: $P_{elec} = U_{RMS}^2/R_{eq}$, with U_{RMS} the RMS voltage.

The output power produced by the harvester for a various types of samara-based propellers is measured, in order to choose the best combination of the three variable parameters: pitch angle, coning angle and number of blades N_b. This leads to an optimal propeller with the following values: $\alpha_p = 30°$, $\beta = 5°$ and $N_b = 8$. The results presented in the following section are those for this propeller.

B. Power and efficiency results

The harvester is tested for air speeds between 1.2 and 8 m.s^{-1}. Its cut-in speed is around 2 m.s^{-1} and when the wind goes down it stops at 1 m.s^{-1}. It produces between 50 μW at 1.2 m.s^{-1} and more than 80 mW at 8 m.s^{-1}. The evolution of electrical output power is illustrated in Fig. 4. It is interesting to note that it follows an exponential trend: there is no concave part that would reflect a fall in efficiency. This phenomenon can be seen in the study by Gasnier et al. for the strongest wind speed of 7 m.s^{-1} [14]. In other words, the harvester keeps here a good efficiency on a large range of wind speeds.

For each wind speed U_0 and according to the value of the resistive load, the rotational frequency of the rotor f changes. This permits to determine the tip-speed ratio λ, defined as the ratio between the speed of the blades tip V_{tip} and the wind speed:

$$\lambda = \frac{V_{tip}}{U_0} = \frac{R.\omega}{U_0} = \frac{R.2\pi.f}{U_0} \tag{3}$$

with R the propeller radius and ω its rotational speed. The overall efficiency of the harvester η is also calculated: $\eta = P_{elec}/P_{air}$. Its evolution for all the wind speeds tested is given in Fig. 5.

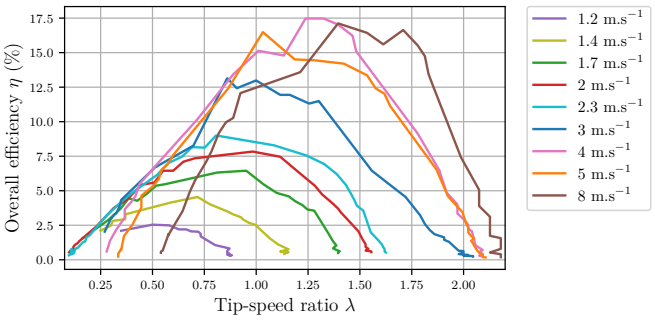

Fig. 5. Overall efficiency as a function of the tip-speed ratio for various wind speeds.

The maximum value of η ranges from 2.5% for a 1.2 m.s^{-1} wind to 17.5% for 4 m.s^{-1}. It increases when the wind speed gets stronger, reaches its maximum at 4 m.s^{-1} and stays around 17% beyond. The optimal tip-speed ratio is between 0.5 and 1.5. The overall efficiency is also plotted as a function of the resistive load on Fig. 6.

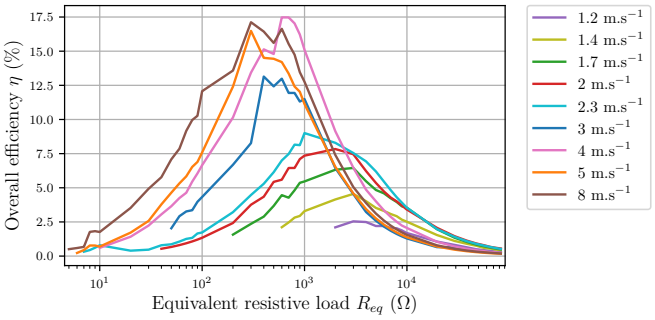

Fig. 6. Overall efficiency as a function of the resistive load for various wind speeds.

It shows that the optimal value of R_{eq} depends on the air speed: it goes down with the wind increasing. Globally, it is situated between 300 and 3000 Ω, with a bandwidth maintaining 90% of the efficiency of about 200 to 300 Ω.

IV. Discussion and conclusion

In terms of maximal overall efficiency, our bioinspired harvester outperforms the ones of the literature with diameters of 7 cm and less [10], [11], [13], [15]–[17], except for the one from Gasnier et al. which demonstrates very high performances [14]. In order to make a deeper comparison, the power density of the harvester is calculated for each wind speed as the ratio between P_{elec} and the rotor area (Fig. 7).

It can be noted that also here, the performances are better than the ones of almost all the existing systems. One interesting point is that the bioinspired harvester covers a large range of wind speeds, from very low to moderate, and that it keeps its performances all the way.

Nevertheless, the efficiency and the power density are the worst at low wind speeds: the work must continue on this point, one way of improvement being to analyze deeper samaras behavior and structure. Another idea to get better performances is to change the material of the generator magnet to NdFeB, which has a higher remanent induction than SmCo and could have a better efficiency, in particular at low air speeds.

References

[1] F. Huet. *Développement de structures hybrides électromécaniques pour micro-sources d'énergie : générateurs piézoélectriques linéaires et non linéaires*. PhD thesis, 2016.

[2] R. K. Singh, M. R. Ahmed, M. A. Zullah, and Y.-H. Lee. Design of a low Reynolds number airfoil for small horizontal axis wind turbines. *Renewable Energy*, 42:66–76, 2012.

[3] R. K. Singh and M. R. Ahmed. Blade design and performance testing of a small wind turbine rotor for low wind speed applications. *Renewable Energy*, 50:812–819, 2013.

[4] S. Bressers, D. Avirovik, C. Vernieri, J. Regan, S. Chappell, M. Hotze, S. Luhman, M. Lallart, D. Inman, and S. Priya. Small-scale modular windmill. *American Ceramic Society Bulletin*, 89(8):34–40, 2010.

[5] R. A. Kishore and S. Priya. Design and experimental verification of a high efficiency small wind energy portable turbine (SWEPT). *Journal of Wind Engineering and Industrial Aerodynamics*, 118:12–19, 2013.

[6] R. A. Kishore, T. Coudron, and S. Priya. Small-scale wind energy portable turbine (SWEPT). *Journal of Wind Engineering and Industrial Aerodynamics*, 116:21–31, 2013.

[7] R. A. Kishore, A. Marin, and S. Priya. Efficient Direct-Drive Small-Scale Low-Speed Wind Turbine. *Energy Harvesting and Systems*, 1(1-2):27–43, 2014.

[8] A. S. Holmes, G. Hong, and K. R. Pullen. Axial-flux permanent magnet machines for micropower generation. *Journal of Microelectromechanical Systems*, 14(1):54–62, 2005.

[9] M. Perez, S. Boisseau, P. Gasnier, J. Willemin, M. Geisler, and J.-L. Reboud. A cm scale electret-based electrostatic wind turbine for low-speed energy harvesting applications. *Smart Materials and Structures*, 25(4):045015, apr 2016.

[10] A. Marin, R. Kishore, D. A. Schaab, D. Vuckovic, and S. Priya. Micro Wind Turbine for Powering Wireless Sensor Nodes. *Energy Harvesting and Systems*, 3(2):139–152, 2016.

[11] D. Carli, D. Brunelli, D. Bertozzi, and L. Benini. A high-efficiency wind-flow energy harvester using micro turbine. *SPEEDAM 2010 - International Symposium on Power Electronics, Electrical Drives, Automation and Motion*, pages 778–783, 2010.

[12] I.-H. Kim, B.-R. Kim, Y.-J. Yang, and S.-J. Jang. Parametric study on ducted micro wind energy harvester. *Energies*, 15(3), 2022.

[13] D. Rancourt, A. Tabesh, and L. Fréchette. Evaluation of centimeter-scale micro windmills: aerodynamics and electromagnetic power generation. *Proc. PowerMEMS*, pages 93–96, 2007.

[14] P. Gasnier, B. Alessandri, T. Fayer, N. Garraud, E. Pauliac-Vaujour, and S. Boisseau. Modelling and Characterization of a High-Efficiency, Cm-Scale and Low Velocity Airflow-Driven Harvester for Autonomous Wireless Sensor Nodes. *Proc. PowerMEMS*, 2019.

[15] P. Gasnier, J. Willemin, S. Boisseau, B. Goubault De Brugière, G. Pillonnet, B. Gomez, and I. Neyret. A cm-scale, low wind velocity and 250°C-compliant airflow-driven harvester for aeronautic applications. *Proc. PowerMEMS*, 2018.

[16] M. Y. Zakaria, D. A. Pereira, and M. R. Hajj. Experimental investigation and performance modeling of centimeter-scale micro-wind turbine energy harvesters. *Journal of Wind Engineering and Industrial Aerodynamics*, 147(September):58–65, 2015.

[17] D. A. Howey, A. Bansal, and A. S. Holmes. Design and performance of a centimetre-scale shrouded wind turbine for energy harvesting. *Smart Materials and Structures*, 20(8):085021, 2011.

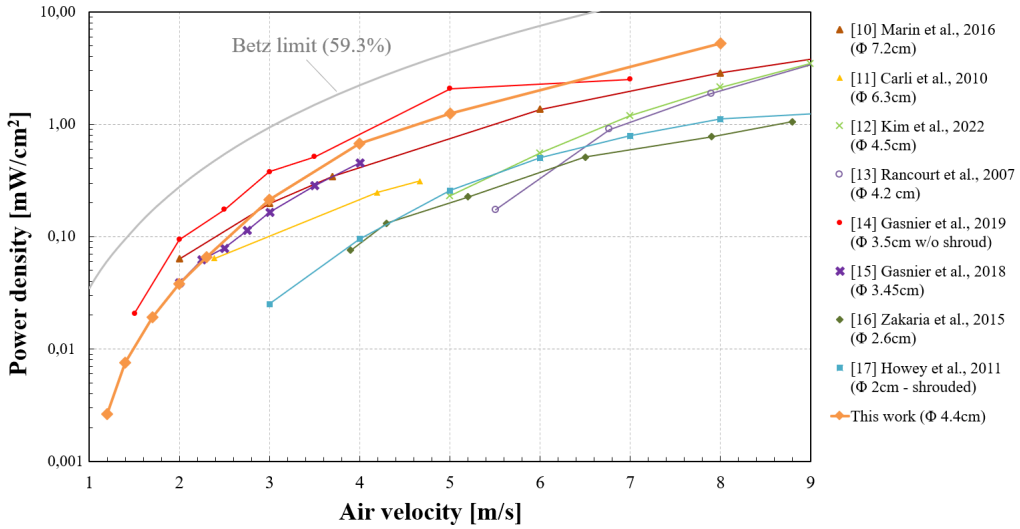

Fig. 7. Power density comparison for centimeter-scale harvesters of the literature (diameter $\leq$ 7 cm).

[18] P. J. Kunz. *Aerodynamics and Design for Ultra-Low Reynolds Number Flight*. PhD thesis, 2003.

[19] J. R. Holden, T. M. Caley, and M. G. Turner. Maple Seed Performance as a Wind Turbine. *53rd AIAA Aerospace Sciences Meeting*, pages 1–14, 2015.

[20] R. A. Norberg. Autorotation, self stability, and structure of single winged fruits and seeds with comparative remarks on animal flight. *Biology Reviews*, 48:561–96, 1973.

[21] R. Nathan, G. G. Katul, H. S. Horn, S. M. Thomas, R. Oren, R. Avissar, S. W. Pacala, and S. A. Levin. Mechanisms of long-distance dispersal of seeds by wind. *Nature*, 418(July):409–414, 2002.

[22] A. Rosen and D. Seter. Vertical Autorotation of a Single-Winged Samara. *Journal of Applied Mechanics*, 58:1064–71, 1991.

[23] D. Lentink, W. B. Dickson, J. L. van Leeuwen, and M. H. Dickinson. Leading-Edge Vortices Elevate Lift of Autorotating Plant Seeds. *Science*, 324:1438–40, 2009.